

Formation behavior and microstructure of multi-cation α -sialons containing neodymium and ytterbium or yttrium

P.L. Wang*, J.H. Zhang, J.B. He, D.S. Yan

*The State Key Lab on High Performance Ceramics and Superfine Microstructure, Shanghai Institute of Ceramics,
Chinese Academy of Sciences, Shanghai 200050, PR China*

Received 27 November 1999; accepted 23 February 2000

Abstract

Multi-cation α -sialons containing neodymium and ytterbium, as well as neodymium and yttrium, were prepared by hot pressing at the temperatures ranging from 1550 to 1750°C for 2 h with the compositions $(\text{Nd}_{0.18}\text{Yb}_{0.18}/\text{Nd}_{0.18}\text{Y}_{0.18})\text{Si}_{10.36}\text{Al}_{1.62}\text{O}_{0.54}\text{N}_{15.46}$. The densification process, reaction sequence, cell dimensions and microstructure were studied in comparison with the corresponding single cation α -sialon. Experimental results have shown that the samples hot-pressed at 1750°C mainly consist of α -sialon phase, whose content (around 95 wt%) is higher than that of counterpart single rare earth doped α -sialon, especially much higher than the one of Nd- α -sialon. On the other hand, the multi-cation α -sialons compositions are beneficial to lower the eutectic temperature in the systems, thus promoting the dissolution of intergranular crystalline melilite phase, and facilitating the precipitation of α -sialon phase. TEM and EDS revealed that the amount of Yb^{3+} or Y^{3+} , which possess relatively smaller ionic radii than Nd^{3+} , is higher than that of the Nd^{3+} in α -sialon grains and more Nd^{3+} are remained in the grain boundary phase. Small amount of elongated α -sialon grains were observed by TEM and the preferred orientation also occurred under hot-pressing for such a low x value composition ($x=0.36$) used in this study. © 2000 Elsevier Science Ltd. All rights reserved.

Keywords: Grain boundaries; Hot pressing; Microstructure-final; Reaction sequence; Sialons

1. Introduction

It is well known that Si_3N_4 -based ceramics are promising materials for high temperature applications due to its outstanding characteristics, such as high temperature strength and good corrosion and wear resistance. On the other hand, solid solution of α - Si_3N_4 , α -sialon (abbreviated as α'), with the general formula $\text{M}_x\text{Si}_{12-(m+n)}\text{Al}_{m+n}\text{O}_n\text{N}_{16-n}$ ($\text{M}=\text{Li}, \text{Ca}, \text{Mg}, \text{Y}$ and part of rare earth elements, i.e. Nd, Sm, Gd, Dy, Er and Yb) has attracted researchers much attentions because α' can incorporate many cations of the additives that are required for densification, thus reducing the amount of residual glass of the material.¹

In the recent years, α' with mixed modifiers,^{2–5} such as Y_2O_3 and M_2O_3 ($\text{M}=\text{La}, \text{Li}, \text{Ca}$),^{2,3} were studied in order to facilitate the densification through lowering the

eutectic temperature of the composition. Several other investigations focused on the incorporation of big cations Ce^{4+} and Sr^{2+} , which do not enter α' structure if it is used alone, together with smaller cations Y_2O_3 and CaO in the α' .^{6–8} In our previous work,⁹ dual cations, Ca^{2+} and Mg^{2+} , were used to form α' ceramics to alleviate the sintering problem of Ca - α' . The results indicated that by use of duplex metal oxide ($0.5\text{CaO} + 0.5\text{MgO}$), instead of CaO , as additives to form α' , the material possessed an improved sintering ability. On the other hand, it was found that the added Ca^{2+} was mainly incorporated into the α' structure, whereas most of the added Mg^{2+} entered sialon polytypoid phase, which imply that the formation behavior of multi-cation α' may differ from single-cation α' .

The similar research work on rare earth is scarce. For single rare earth cation α' , which has been most extensively studied because of the high refractoriness of their boundary glass, several studies^{10–12} have reported the reaction process and phase assembly. The work on densification behavior of R - α' ($\text{R}=\text{Nd}, \text{Sm}, \text{Gd}, \text{Dy}, \text{Er}$ and Yb)¹² indicated that hot-pressing temperatures,

* Corresponding author. Tel.: +86-21-6251-2990; fax: +86-21-6251-3903.

E-mail address: plwang@sunm.shcnc.ac.cn (P.L. Wang).

which were necessary to get fully densified samples, decreased with increasing the atomic number of rare earth elements, as shown in Fig. 1. The reaction sequences of Nd-, Y- and Yb- α' ,¹² shown in Fig. 2 (a)–(c), revealed that the α' content was higher in heavy rare earth-doped α' than in light rare earth- α' , whereas crystalline grain boundary melilite (actually, it was melilite solid solution, $R_2Si_{3-x}Al_xO_{3+x}N_{4-x}$, abbreviated as M') phase possessed an opposite formation tendency of α' . These results reflect the effect of type of rare earth on densification, reaction sequence and final phase assemblage for rare earth- α' compositions. Therefore, the study of sintering and formation behavior of dual cations α' , composed of light and heavy rare earth ions, would be interesting. The present work involves the formation behavior of multi-cation α' containing neodymium and yttrium. The same composition for neodymium and

yttrium doped α' is also studied as a comparison. The effects of mixed modifiers on microstructure and cations distribution in the final products have been investigated too.

2. Experimental

In the previous work¹² on the formation behavior of rare earth(R)- α' (R = Nd, Sm, Gd, Dy, Er and Yb), the compositions $R_{0.36}Si_{10.36}Al_{1.62}O_{0.54}N_{15.46}$, which is along the tie line between Si_3N_4 and $R_2O_3 \cdot 9AlN$ with x equal to 0.36, were used. In order to compare the results with R- α' , the similar compositions $Nd_{0.18}Yb(Y)_{0.18}Si_{10.36}Al_{1.62}O_{0.54}N_{15.46}$ were selected for multi-cation α' -sialons containing (Nd + Yb) and (Nd + Y), respectively, in the present study. The starting powders used were Si_3N_4 (UBE-10, Japan, 2.0 wt%O), AlN (1.3 wt%O), Al_2O_3 (CR30, Wusong Chemical Plant, China, 99.5%), R_2O_3 (R = Nd, Y and Yb, Yaolung Chemical Plants, China, 99.9%). The powders were milled under absolute alcohol for 48 h in a plastic jar, using sialon milling media. Pellets of dried powders were hot-pressed under nitrogen atmosphere in a graphite resistance furnace at temperatures ranging from 1550 to 1750°C for 2h.

The bulk densities of the samples were measured by the Archimedes principle. Phase assemblages were characterized by XRD using a Guinier-Hägg camera with $Cu K\alpha_1$ radiation and Si as an internal standard. The measurement of X-ray film and refinement of lattice parameters were completed by a computer-linked line scanner (LS-18) system¹³ and the program PIRUM¹⁴ respectively. XRD patterns of the samples were also obtained by diffractometer with $Cu K\alpha$ radiation on the surface perpendicular to hot-pressing direction to study the preferred orientation of α' grains. The semi-quantitative estimation of the crystalline phases of samples

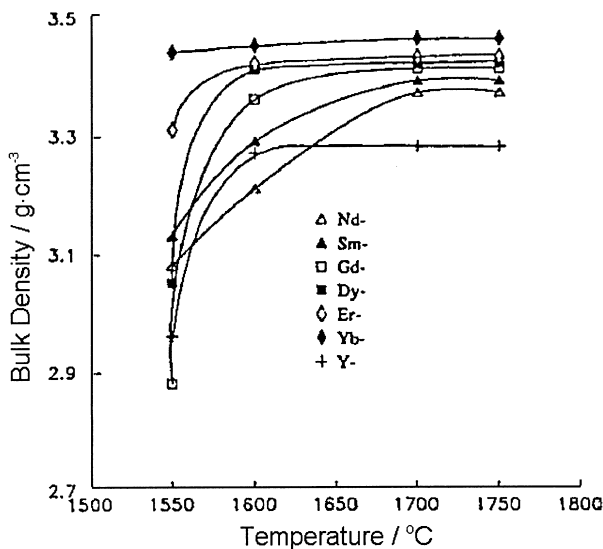


Fig. 1. Densification behaviour of R(Y)- α -sialon compositions by hot-pressing.¹²

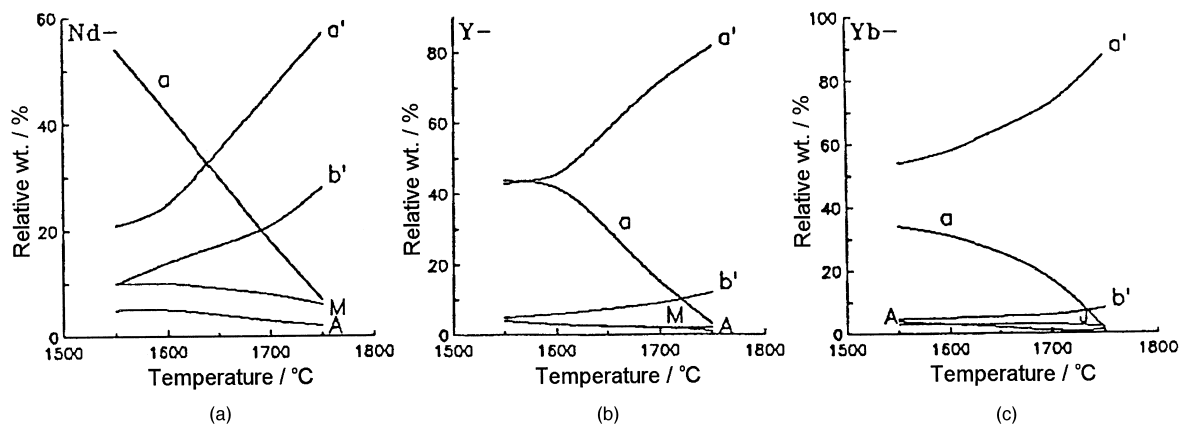


Fig. 2. Reaction sequences of (a) Nd- α -sialon, (b) Y- α -sialon, (c) Yb- α -sialon compositions ($x=0.36$) during hot-pressing.¹² a, α - Si_3N_4 ; a', α -sialon; b', β -sialon; M, melilite (see text); A, AlN.

was based on the calibration curves obtained from appropriate powder mixtures of every two phases. Microstructure observation was performed in the samples hot-pressed at 1750°C under a transmission electron microscope JEM 200CX equipped with a linked ISIS 3.00 EDX system. The TEM samples were coated with a thin evaporated carbon film to minimize electron beam charge.

3. Results and discussion

3.1. Densification and reaction sequence

The densification process of (Nd + Yb)- and (Nd + Y)- α' compositions can be estimated from the curves of bulk density vs sintering temperature as shown in Fig. 3. The figure shows that density of (Nd + Yb)- α' sample is higher than that of (Nd + Y)- α' at all investigated temperatures. According to the study on densification of R- α' ,¹² the lowest shrinkage temperature among R- α' occurs at 1490°C for Yb- α' composition, while at about 1550°C for other- α' samples. It is founded in present work that the shrinkage temperature is between 1490 and 1550°C for (Nd + Yb)- and 1550°C for (Nd + Y)- α' compositions, respectively, thus resulting in the higher densification of former sample than the latter one. It is also noted that the hot-pressing temperature for fully densification of (Nd + Yb)- α' composition is 1650°C, which is 50°C lower than the one of (Nd + Y)- α' .

The reaction sequences of (Nd + Yb)- α' and (Nd + Y)- α' compositions are shown in Fig. 4 (a) and (b), which are mostly alike as seen from the figures. At 1550°C, substantial amount of M' phase (~10 wt%) has been formed along with α' phase (> 30 wt%). With temperature increasing, the content of α' phase increases at the

expense of α -Si₃N₄, AlN and previously formed M'. The unreacted α -Si₃N₄ disappears at 1700°C for (Nd + Yb)- α' composition and remains with trace amount until 1750°C for (Nd + Y)- α' composition. M' phase is founded in all hot-pressing temperatures for two compositions, however, remaining with very small amount in the final products. As shown in Fig. 4, the amount of α' is smaller in (Nd + Y)- α' composition than that of (Nd + Yb)- α' in most sintering temperatures, except 1550°C. Besides α' and M', the samples also contain a small amount of β -sialon (β').

Based on the results shown in Figs. 3 and 4 and the previous work¹² shown in Figs. 1 and 2, it is founded that there exist several obvious differences between multi-cation α' and single-cation α' compositions for the densification and formation behavior. First, different from R- α' , the densification process of (Nd + Yb)- and (Nd + Y)- α' compositions is almost synchronous with reaction sequence. The α' content for (Nd + Y)- α' composition has already increased to 89 wt% at 1700°C, when the densification process is nearly completed. In (Nd + Yb)- α' case, α' content reaches 86 wt% at 1650°C, at which the sample is almost densified. However, the reaction of single cation R- α' compositions do not fully complete when the bulk densities of R- α' samples has reached their maximum values. For example, as shown

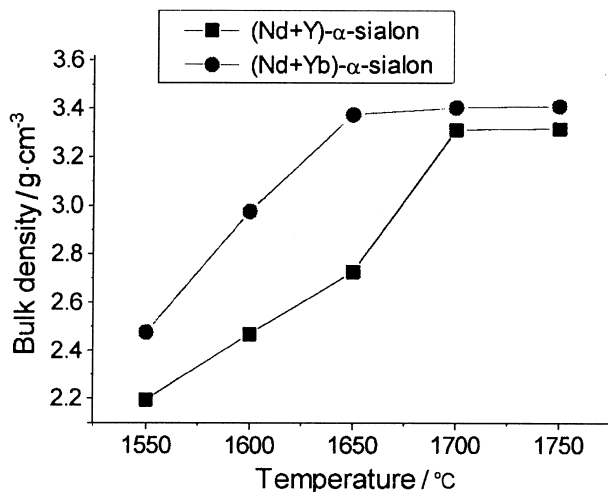


Fig. 3. Densification behaviour of (Nd + Yb)- α -sialon and (Nd + Y)- α -sialon compositions by hot-pressing.

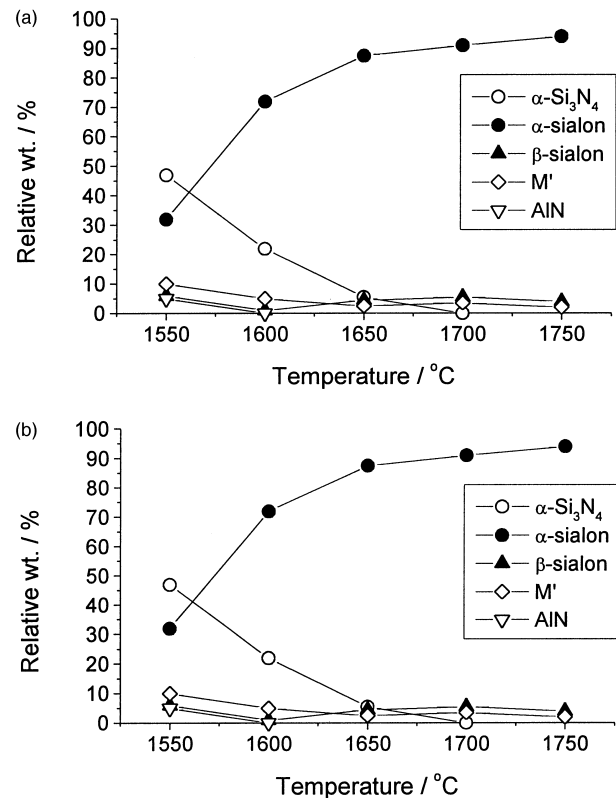


Fig. 4. Reaction sequences of (a) (Nd + Yb)- α -sialon composition ($x=0.36$), (b) (Nd + Y)- α -sialon composition ($x=0.36$) during hot-pressing.

in Figs. 1 and 2, 1550, 1600 and 1700°C are necessary for fully densification of Yb-, Y- and Nd- α' compositions respectively and the corresponding α' contents at these temperatures are respectively around 55, 45 and 45 wt%. Second, the α' contents in both (Nd+Yb)- and (Nd+Y)- α' compositions are higher than that of R- α' (R = Nd, Y and Yb) compositions at all sintering temperatures except 1550°C for Y- α' and 1550, 1600°C for Yb- α' compositions (see Figs. 2 and 4). The amount of α' phase can reach up to around 95 wt% in the final products when α' is doped with multi-cation rare earth ions as the present work, whereas it is less than 60 wt% for Nd- α' composition. Consequently, the amounts of β' and M' phases are decreased in multi-cation α' samples, in comparison with single cation α' case. As seen from Fig. 2, the corresponding amounts in the final products are around 8 wt% of M' and 28 wt% of β' for Nd- α' composition, 2 wt% of M' and 12 wt% of β' for Y- α' composition. For Yb- α' composition, instead of M', crystalline J phase ($\text{Yb}_4\text{Si}_2\text{O}_7\text{N}_2$) appeared in the reaction sequence and the amounts of J phase and β' are respectively about 2 and 8 wt%. On the other hand, the estimated amounts of 2 wt% of M' and 5 wt% of β' for both (Nd+Yb)- and (Nd+Y)- α' compositions sintered at 1750°C are obtained based on Fig. 4 (a) and (b).

Densification and formation behavior of α' are closely related to the amount and viscosity of liquid present in sintering process. For the different rare earth containing α' compositions, increasing temperature may have different effects on the reaction process and liquid formation. At the beginning of sintering, i.e. at relatively low temperature, the sample may be densified without completing the reaction if a large amounts of liquid have already been present, like the Yb- α' case.¹² As to (Nd+Yb)- and (Nd+Y)- α' samples, the reaction process occur nearly simultaneous with densification process, which suggests that the processes of liquid formation and reaction are almost concurrent with increasing the temperature. It is also noticed that, in the incipient sintering stage, multi-cation α' exhibits relative lower density than Yb- and Y- α' . The cause of this may be the fact that relative higher content of α' and M' formed in that stage for multi-cation α' samples than for R- α' compositions, which absorbs large amounts of rare-earth ions and hence, hinders the densification process.

It can be seen from Figs. 2 and 4 that the amounts of M' phase at 1550°C in (Nd+Yb)-, (Nd+Y)- and Nd- α' samples are similar. It is, however, reduced in former two samples with increasing the sintering temperatures, whereas almost remaining at the same level until 1750°C in Nd- α' sample. The latter result indicates that the M' phase has not been dissolved into the liquid even at 1750°C in Nd- α' system and, consequently, less α' is formed. For multi-cation α' , the use of mixture of light and heavy rare earth oxides is beneficial to lower the eutectic temperature in the systems, however, thus

promoting the dissolution of intergranular crystalline M' phase into the liquid during reaction sequence and facilitating the precipitation of α' phase. The formation of β' phase is curbed at the same time. It is expected that multi-cation α' materials would possess a better comprehensive property than single cation α' because of less grain boundary phase contained.

3.2. Cell dimensions of α' phase

To further understand the reaction kinetics of the (Nd+Yb)- and (Nd+Y)- α' , the cell dimensions of α' phase were determined and plotted in Fig. 5. As known, the formation of α' is a process of solution and precipitation. Part of $\alpha\text{-Si}_3\text{N}_4$ absorbs the rare earth ions from the liquid to be precipitated to form α' at low temperature ($\sim 1550^\circ\text{C}$). With temperature increasing ($\sim 1600^\circ\text{C}$), more amounts of liquid emerge and $\alpha\text{-Si}_3\text{N}_4$ continue to react and form α' . It is noticed that the largest cell dimensions of α' phase occur at 1600°C among the whole reaction temperatures for both (Nd+Yb)- α' and (Nd+Y)- α' . This is considered to be resulted from the more M' phase dissolved for (Nd+Yb)- α' and relatively lower amount of α' phase formed for (Nd+Y)- α' sample at this temperature (see Fig. 4). It is well known that the lattice parameters of α' expand when more cations are absorbed into the α' structure. Therefore, the highest lattice parameters of α' indicate that formed α' phase absorbs largest amounts of rare-earth ions at this temperature although the reaction is not completed at this stage. With temperature further increasing, liquid significantly emerges, consequently more α' phase is formed. The fact that the cell dimensions of α' phase in multi-cation α' compositions decrease when the sintering temperatures are higher than 1600°C, suggests that the α' grains may be re-dissolved into the liquid and then the rare-earth ions are redistributed, while large amounts of α' are formed at higher sintering temperatures. It is also noticed that the lattice parameters of (Nd+Yb)- α' phase are obviously larger than that of

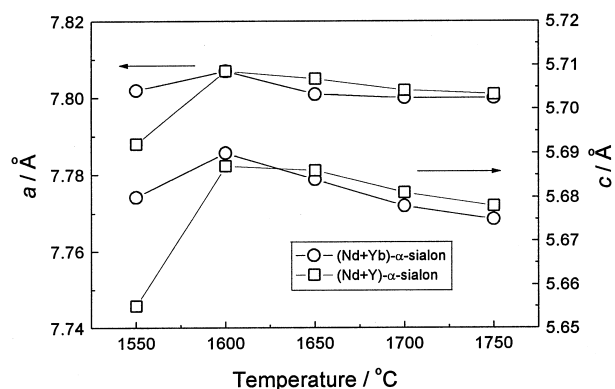


Fig. 5. Cell dimensions of (Nd+Yb)- α -sialon and (Nd+Y)- α -sialon vs sintering temperature.

(Nd+Y)- α' phase at 1550°C, as shown in Fig. 5, which implies that (Nd+Yb) ions than (Nd+Y) ions are more easily to enter α' structure at this temperature. The cause of this is attributed to the relatively more amounts of liquid phase formed in (Nd+Yb)- α' than (Nd+Y)- α' as the density of the former sample at 1550°C is obviously higher than the latter one. When the sintering temperatures are higher than 1600°C, the lattice parameters of (Nd+Y)- α' are little larger than the corresponding ones of (Nd+Yb)- α' , which are resulted from the difference of ionic radii between Y^{3+} (0.89 Å) and Yb^{3+} ions (0.86 Å).

3.3. Microstructural features

TEM photographs of (Nd+Yb)- α' and (Nd+Y)- α' compositions are shown in Figs. 6 and 7, respectively. TEM observation indicates that the morphologies of

(Nd+Yb)- α' and (Nd+Y)- α' are similar. The microstructure consists of mostly equi-axed or nearly equi-axed α' grains (0.2–1.0 μm), which are adjoined by thin glassy films and tri-angle grain boundary with glassy phase (10–200 nm). EDS analysis was performed on both the α' grains and the grain boundary glassy phase. The results have shown that in α' grains the amount of Yb(Y) is higher than that of Nd and the ratios of Yb to Nd and Y to Nd are around 2 and 2.5 for (Nd+Yb)- and (Nd+Y)- α' grains, respectively, which reveal that rare earth ion with smaller ionic radius is easier to enter into α' structure. On the other hand, EDS analysis for intergranular rare phase indicates that there exist larger amounts of rare-earth ions in the grain boundary than in the α' grains, different from α' grains, in which the amount of Nd is higher than the one of Yb(Y). Consistent with the results of Ekström et al.⁷ this observation suggests that in mixed- R_2O_3 doped α' , the smaller rare

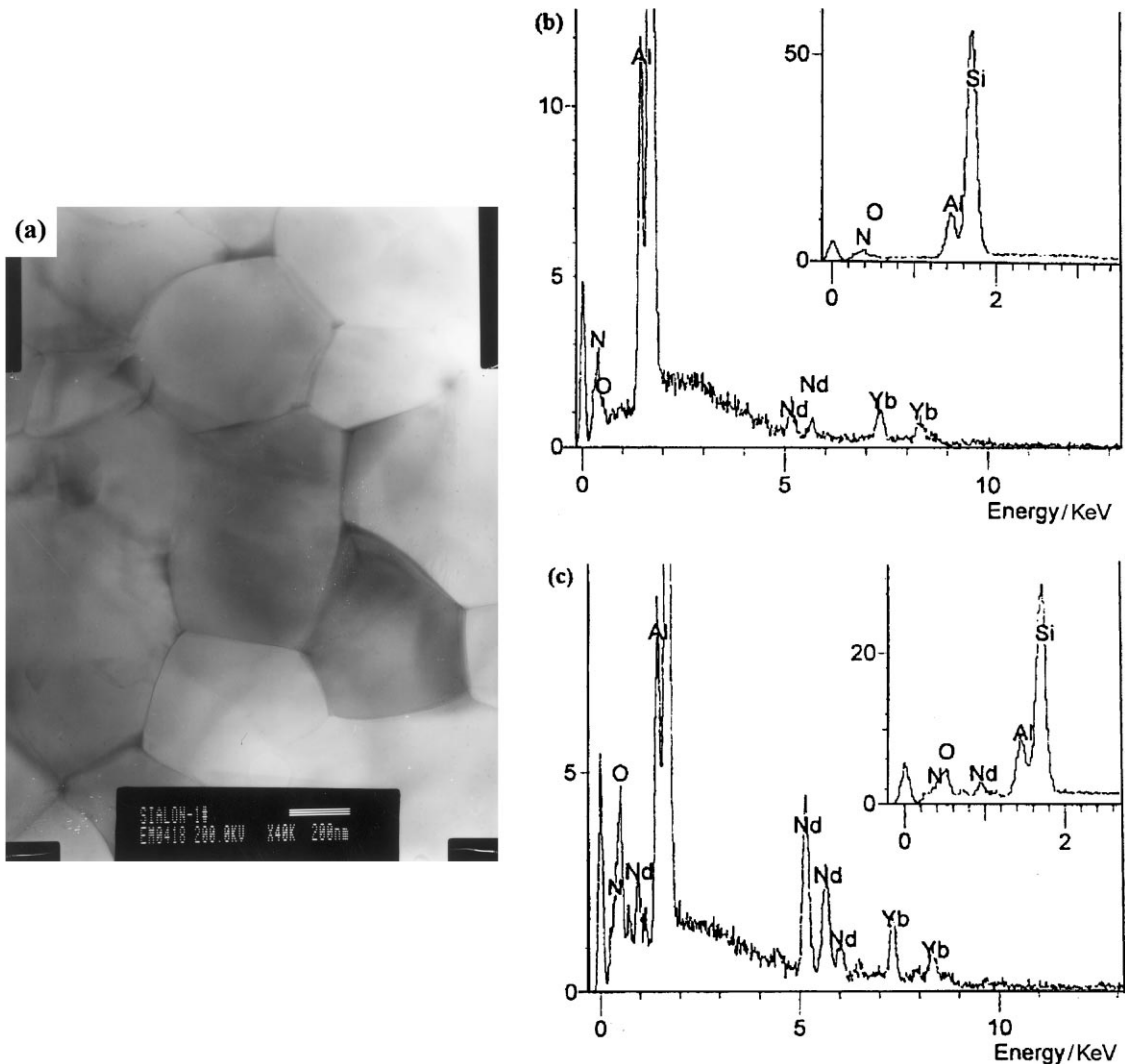


Fig. 6. (a) TEM bright-field image of (Nd+Yb)- α -sialon; (b) a typical EDS pattern of the equi-axed α -sialon grains in (a); (c) a typical EDS pattern of intergranular phase in (a) Note: the Yb:Nd ratio changes from ~ 2 in α -sialon grain to ~ 0.6 in the intergranular phase.

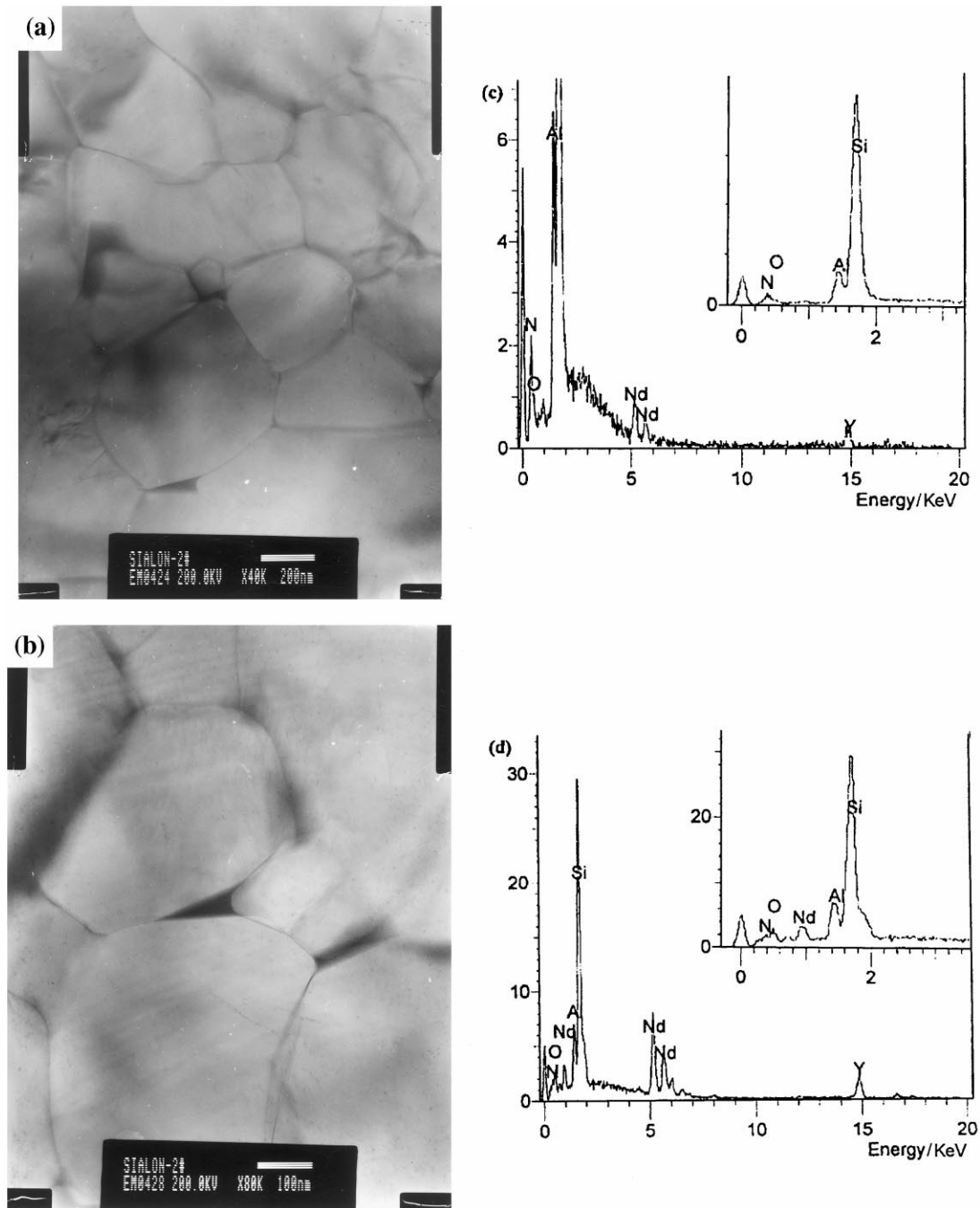


Fig. 7. Two TEM bright-field images of (Nd+Y)- α -sialon in (a) and (b); (c) a typical EDS pattern of the equiaxed α -sialon grains in (a); (d) a typical EDS pattern of intergranular phase in (b). Note: the Y:Nd ratio changes from ~2.5 in α -sialon grain to ~0.3 in the intergranular phase.

earth ions Yb^{3+} (Y^{3+}) enter more easily into the α' structure than the larger Nd^{3+} .

It has been known that β' grains are easy to develop into aciculate and therefore, its fracture toughness is relatively high. On the other hand, α' exhibits equiaxed morphology with low fracture toughness. However, α -sialon with elongated grain morphology has been reported by several studies^{8,15–19} in the recent years. Hwang et al.⁸ and Wang et al.¹⁵ observed the preferred orientation of α' grains in hot-pressing samples for

($\text{Y}_2\text{O}_3/\text{SrO}/\text{CaO}$) and CaO doped α/α' systems respectively. The new results^{16–19} revealed that α' can develop into aciculate morphology under suitable conditions. The Stockholm work^{16,17} indicated that in the Ln-Si-Al-O-N system, the liquid phase promotes the formation of elongated α' . Chen et al.¹⁸ reported that the elongated Ln- α -sialon grains are more easily to occur by using β - Si_3N_4 as starting materials (normally α - Si_3N_4 as starting materials) and Hewett et al.¹⁹ reported the occurrence of elongated Ca- α -sialon grains in the

Table 1
XRD peak height ratios of (210)/(102) in (Nd + Yb)- and (Nd + Y)- α' -sialons^a

Peak ratio	(Nd + Yb)- α' (HP)*	(Nd + Yb)- α' (P)*	(Nd + Y)- α' (HP)	(Nd + Y)- α' (P)
(210)/(102)	2.17	0.93	3.39	0.81

^a HP, XRD pattern of the surface perpendicular to the hot-press axis; P, XRD pattern of pulverised sample.

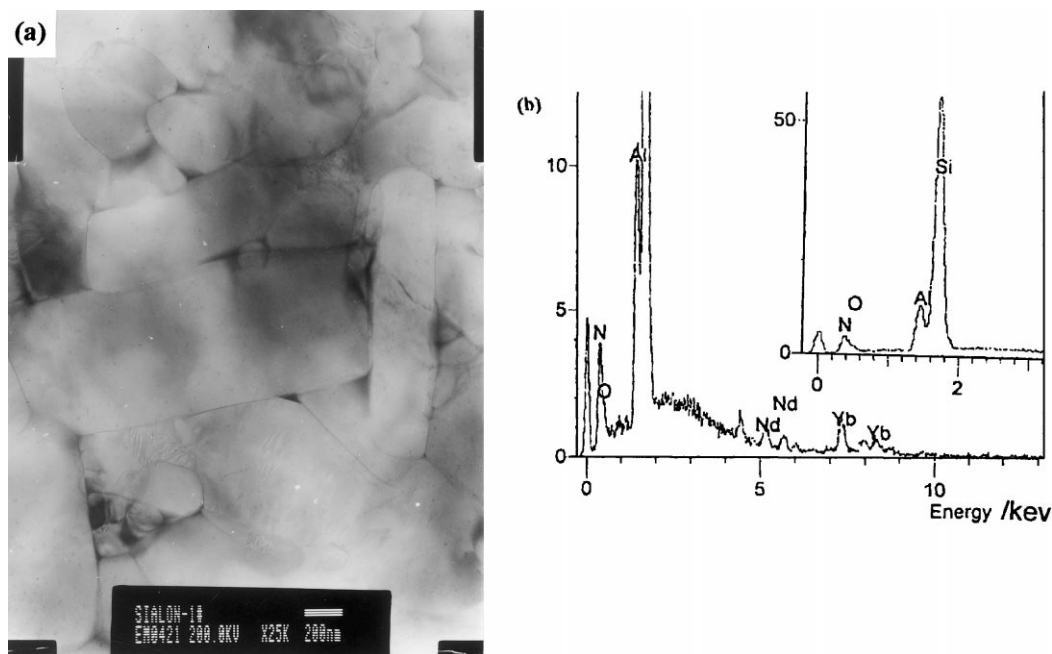


Fig. 8. (a) TEM bright-field image showing α' -sialon grains with elongated morphology in (Nd + Yb)- α' -sialon; (b) a typical EDS pattern of the elongated α' -sialon grains.

Ca–Al–Si–O–N system. In the present work, XRD patterns of (Nd + Yb)- and (Nd + Y)- α' samples were determined by both diffractometer (on the surface normal to hot-pressing direction) and Guiner-Hägg camera. The former pattern showed a strong evidence for the preferred orientation of α' grains since the diffraction intensity of (210) peak is higher than the one of (102) for both (Nd + Yb)- and (Nd + Y)- α' samples as listed in Table 1. On the other hand, no preferred orientation occurs in the latter pattern as the film was taken by using powder. It is thought that the elongated α' grains will give preferred orientation under hot-pressing, it is therefore believed that the elongated α' grains would occur in the (Nd + Yb)- and (Nd + Y)- α' samples. By TEM, the elongated α' grains were observed, in which the grains possess more than 1 μm in length with aspect ratio more than 3, as shown in Fig. 8 and 9 for (Nd + Yb)- and (Nd + Y)- α' samples respectively. The corresponding EDS analyses for the grains further confirmed that it was the α' phase as the elements distributions were similar to the ones of α' grains with equi-axed morphology [see Fig. 8 (b) and 9 (b)]. Very small amount

of β' grains were also observed by TEM as shown in Fig. 9(c). The confirmation of β' grain was made by no rare earth elements detected with EDS. Based on the reported work on the formation of elongated α' grains using α - Si_3N_4 as starting material,^{15–17,19} the compositions used all had high x values ($x \geq 1.0$), which is beneficial to form more liquid phase during sintering and to develop α' grains into elongated morphology. In our previous work for Ca- α' ,²⁰ it was also found that with the compositions shifting to the low x value, like $x = 0.6$, of the compositions, the α' grains become smaller and less elongated grains appear. However, the preferred orientation do occur for the composition ($x = 0.36$) used in the present work, which is close to the lowest limit ($x = 0.33$) of solubility for rare earth in α' . Therefore, it is considered that most α' grains in multi-cation α' possess equi-axed or nearly equi-axed α' morphology as mentioned above. However, the grains with nearly equi-axed morphology actually have low aspect ratio and the preferred orientation in (Nd + Yb)- and (Nd + Y)- α' samples are due to the contribution of both elongated or nearly equi-axed with low aspect ratio α' grains.

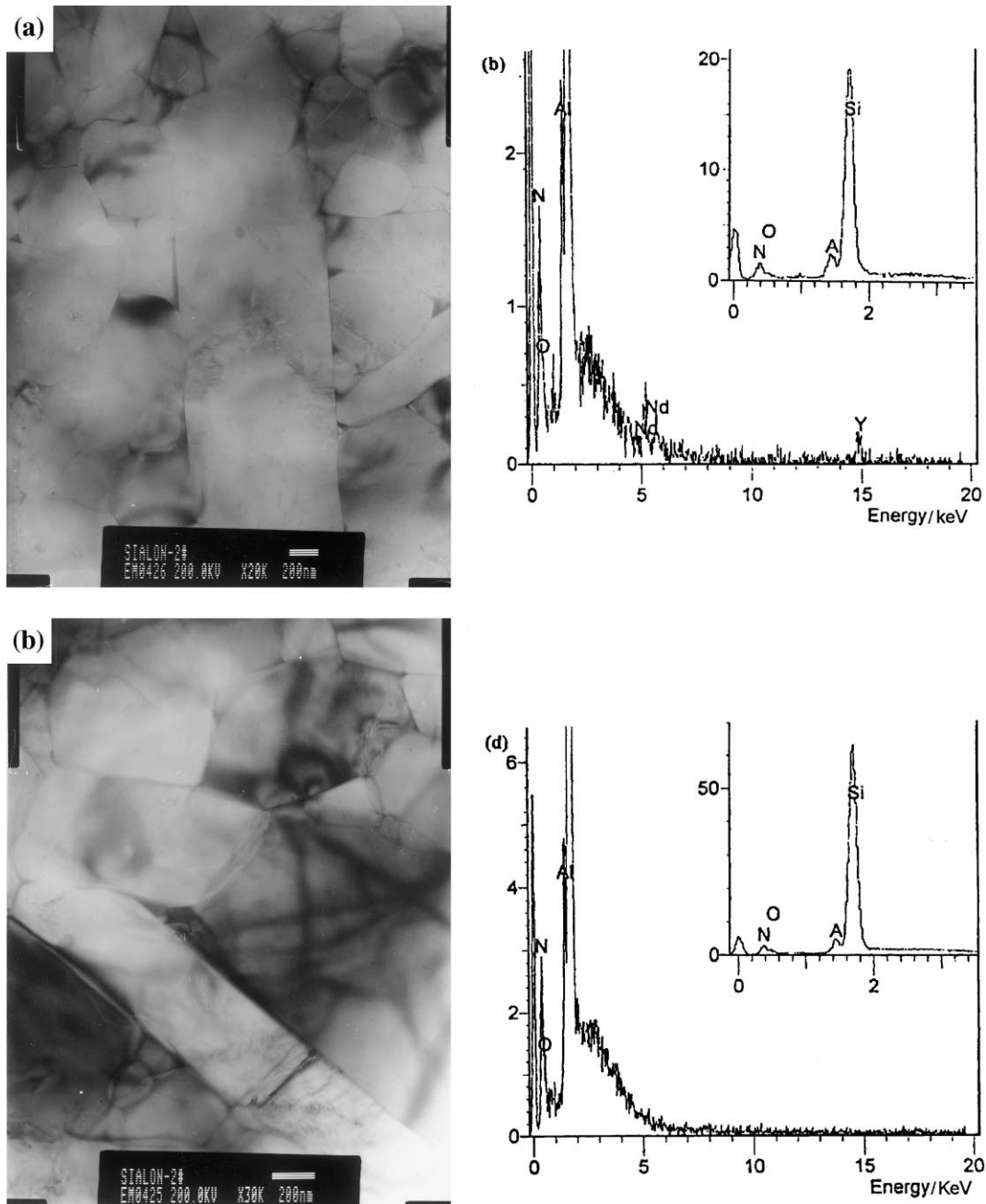


Fig. 9. (a) TEM bright-field image showing α -sialon grains with elongated morphology in (Nd+Y)- α -sialon; (b) a typical EDS pattern of the elongated α -sialon grains; (c) TEM bright-field image showing an acicular β -sialon grain in (Nd+Y)- α -sialon composition; (d) EDS pattern of the β -sialon grain.

4. Conclusions

1. The densification process is completed by hot-pressing at 1650°C for (Nd+Yb)- α' and 1700°C for (Nd+Y)- α' compositions. The reaction sequences of the (Nd+Yb)- α' and (Nd+Y)- α' are nearly simultaneous with the densification process.

2. The (Nd+Yb)- and (Nd+Y)- α' compositions hot-pressed at 1750°C mainly consists of α' phase, whose content (around 95 wt%) is higher than that of

counterpart single rare earth doped α' compositions, especially much higher than the one of Nd- α' . On the other hand, the use of mixture of light and heavy rare earth oxides in the compositions is beneficial to lower the eutectic temperature in the systems, thus promoting the dissolution of intergranular crystalline M' phase into the liquid during reaction sequence and facilitating the precipitation of α' phase.

3. The largest lattice parameters of α' phase occur at 1600°C among the whole reaction temperatures for both

(Nd + Yb)- α' and (Nd + Y)- α' . The cell dimensions of α' phase decrease when the sintering temperatures are higher than 1600°C, indicates that the α' grains may be re-dissolved into the liquid and then the rare-earth ions are redistributed, while large amounts of α' are formed at higher sintering temperatures.

4. In multi-cation (Nd + Yb)- and (Nd + Y)- α' samples, smaller rare earth ions Yb^{3+} (Y^{3+}) enter more easily into the α' structure than the larger Nd^{3+} . Therefore, Yb^{3+} (Y^{3+}) content is higher than that of Nd^{3+} in α' grain. On the other hand, more Nd^{3+} are founded in the grain boundary phase of the materials.

5. The preferred orientation also occurred under hot-pressing for such a low x value composition ($x=0.36$) used in this study, which is considered as the contribution of α' grains with both morphologies, elongated or nearly equi-axed with low aspect ratio.

Acknowledgements

This work was supported by National Natural Science Foundation of China.

References

- Hampshire, S., Park, H. K., Thompson, D. P. and Jack, K. H., α' -Sialon ceramics. *Nature*, 1978, **274**, 880–882.
- Olsson, P.-O. and Ekström, T., HIP-sintered β - and mixed α - β sialons densified with Y_2O_3 and La_2O_3 additions. *J. Mater. Sci.*, 1990, **25**, 1824–1832.
- Huang, Z. K., Jiang, Y. Z. and Tien, T. Y., Formation of α -sialons with dual modifying cations (Li + Y and Ca + Y). *J. Mater. Sci. Lett.*, 1997, **16**, 747–751.
- Kall, P.-O. and Ekström, T., Sialon ceramics made with mixtures of Y_2O_3 - Nd_2O_3 as sintering aids. *J. Eur. Ceram. Soc.*, 1990, **6**, 119–127.
- Redington, M. and Hampshire, S., Multi-cation α -sialons. *Br. Ceram. Proc.*, 1992, **49**, 175–190.
- Olsson, P.-O., Crystal defects and coherent intergrowth of α - and β -crystals in Y-Ce doped sialon materials. *J. Mater. Sci.*, 1989, **24**, 3878–3887.
- Ekström, T., Jansson, K., Olsson, P.-O. and Persson, J., Formation of an Y/Ce-doped α -sialon phase. *J. Eur. Ceram. Soc.*, 1991, **8**, 3–9.
- Hwang, C. J., Susnitzky, D. W. and Beaman, D. R., Preparation of multication α -sialon containing strontium. *J. Am. Ceram. Soc.*, 1995, **78**, 588–592.
- Wang, P. L., Zhang, C., Sun, W. Y. and Yan, D. S., Formation behavior of multi-cation α -sialons containing calcium and magnesium. *Materials Letters*, 1999, **38**, 178–185.
- Shen, Z. J., Ekström, T. and Nygren, M., Homogeneity region and thermal stability of neodymium doped α -sialon ceramics. *J. Am. Ceram. Soc.*, 1996, **79**, 721–732.
- Cheng, Y.-B. and Thompson, D. P., Preparation and grain boundary devitrification of samarium α -sialon ceramics. *J. Eur. Ceram. Soc.*, 1994, **14**, 13–21.
- Wang, P. L., Sun, W. Y. and Yen, T. S., Sintering and formation behavior of R- α' -Sialons (R = Nd, Sm, Gd, Dy, Er and Yb). *Eur. J. Solid State Inorg. Chem.*, 1994, **31**, 93–104.
- Johansson, K. E., Palm, T. and Werner, P.-E., An automatic microdensitometer for x-ray powder diffraction photographs. *J. Phys. E.: Sci. Instrum.*, 1980, **13**, 1289–1291.
- Werner, P.-E., A fortran program for least-squares refinement of crystal-structure cell dimensions. *Arkiv für Kemi.*, 1964, **31**, 513–516.
- Wang, H., Cheng, Y.-B., Muddle, B. C., Gao, L. and Yen, T. S., Preferred orientation in hot-pressed Ca α -sialon ceramics. *J. Mater. Sci. Lett.*, 1996, **15**, 1447–1449.
- Shen, Z. J., Nordberg, L.-O., Nygren, M. & Ekström, T., α -Sialon grains with high aspect ratio-utopia or reality? In *Proc. Nato AST Engineering Ceramics 96 — Higher Reliability through Processing*, ed. G. N. Babini et al. Kluwer Academic, Dordrecht, 1997, pp.169–178.
- Nordberg, L.-O., Shen, Z., Nygren, M. and Ekström, T., On the extension of the α -sialon solid solution range and anisotropic grain growth in Sm-doped α -sialon ceramics. *J. Eur. Ceram. Soc.*, 1997, **17**, 575–580.
- Chen, I.-W. and Rosenflanz, A., A tough SIALON ceramics based on α - Si_3N_4 with a whisker-like microstructure. *Nature*, 1997, **389**, 701–704.
- Hewett, C. L., Cheng, Y. B., Muddle, B. C. and Trigg, M. B., Phase relationships and related microstructural observations in the Ca–Si–Al–O–N system. *J. Am. Ceram. Soc.*, 1998, **81**, 1781–1788.
- Wang, P. L., Zhang, C., Sun, W. Y. and Yan, D. S., Characteristics of Ca- α -sialons—phase formation, microstructure and mechanical properties. *J. Eur. Ceram. Soc.*, 1999, **19**, 553–560.